Available online at www.sciencedirect.com
ScienceDirect
Journal of the European Ceramic Society 30 (2010) 2971–2975
www.elsevier.com/locate/jeurceramsoc

Bubble-free electrophoretic shaping from aqueous suspension with micro point-electrode

A. Nold*, R. Clasen

Saarland University, Bldg. C6 3, 66123 Saarbrücken, Germany

Available online 4 April 2010

Abstract

The electrophoretic deposition (EPD) is a well-suited process for shaping compacts of nanosized powders. Aqueous suspensions are favorable for industrial application due to the high polarity of water enabling high solid loadings and for environmental reasons. Moreover, for many applications a local deposition is of interest. In this case the electric field has to be focused on a small point. This is a problematic issue when the aqueous suspension has a high electrical conductivity.

The local resolution of the deposition was improved by moving both electrodes closer to each other. The limiting factor was the formation of bubbles by water electrolysis, which disturb the electric field at the electrodes. Therefore the electric field distribution of several electrode-configurations was calculated and the most suitable setup was selected. The formation of bubbles was suppressed by using unbalanced pulses of alternating voltage. Point deposits with diameter smaller than 740 μm were obtained, which were only about 1.5 times larger than the point electrode diameter. Possible applications of this technique in the future are rapid prototyping or commercial manufacturing of individual structures like those required in the dental industry.

Keywords: EPD; Shaping; Defects; Al_2O_3; Structural applications

1. Introduction

The electrophoretic deposition (EPD) is an interesting and versatile process for shaping compacts, especially for nano-sized powders. Compacts of nanopowders can be completely sintered at much lower temperatures than those obtained with conventional micron powders, if a comparable green density is achieved. Aqueous suspensions are favorable for industrial applications due to the high polarity of water enabling high solid loadings and for environmental reasons. For many applications a local deposition is of interest. For that the electric field has to be focused on a small point. This is a problematic issue when working with aqueous suspensions of high electrical conductivity.

Our previous works[1–4] showed the possibility of the EPD-process as a rapid prototyping technique. However, the size of the previous structured deposits was in the millimeter range. But for many applications smaller structures are of interest. In order to reduce the size of the deposit, the electric field must be focused more closely. This can be achieved using finer point electrodes and reducing the distance between them. In aqueous suspensions the problem of the bubble formation at the electrodes due to the water decomposition has to be solved. In our previous work, the EPD membrane configuration was used to prevent bubbles being incorporated into the deposit.[5,6] As the point electrodes were farther apart from each other the gas bubbles could freely rise towards the surface of the suspension.[7] Thus bubble-free deposits were obtained. But at a reduction of the distance between the electrodes the formation of a gas bubble on the surface of the point electrode disturbs the local electric field. Therefore a bubble formation has to be completely suppressed at both electrodes.

The bubble formation can be reduced by applying chemical additives.[8,9] However, such solutions do not work with point electrodes with high current densities. Furthermore, one additive can suppress the bubble formation only at one electrode. It is well known, that water electrolysis is promoted whenever the required decomposition voltage is applied, leading to bubbles formation. More specifically, at the electrode surface occurs a heterogeneous-nucleation and bubble-growth process. For the latter, a critical concentration of bubble-forming precursors is required. Dinkelacker[10] (Fig. 1) reported the required time as

* Corresponding author.
E-mail address: a.nold@nanotech.uni-saarland.de (A. Nold).

0955-2219/$ – see front matter © 2010 Elsevier Ltd. All rights reserved.
doi:10.1016/j.jeurceramsoc.2010.03.005

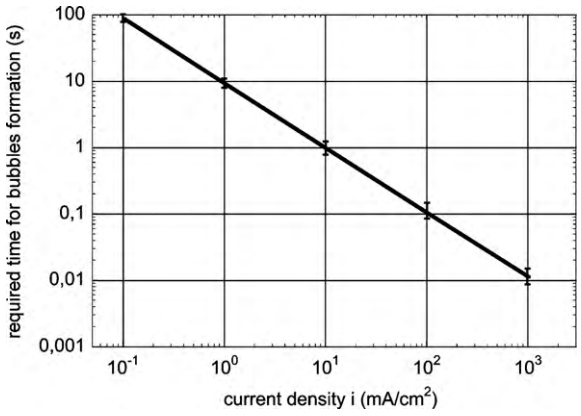

Fig. 1. Time for bubbles formation as a function of current density.[10]

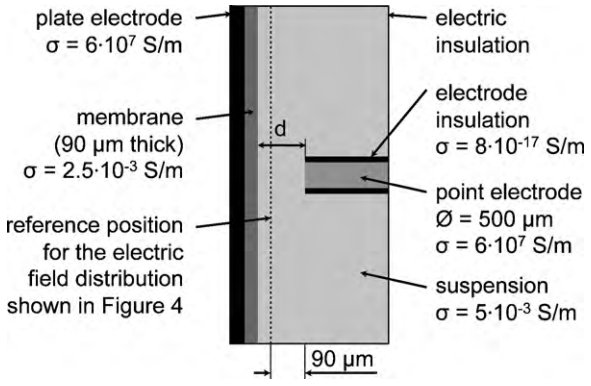

Fig. 2. Setup for simulating electric fields.

a function of the current density for the formation of bubbles. At low current densities no bubbles are produced, as the precursors diffuse back into the bulk of the electrolyte. As the current density is increased, the required time to bubbles formation is consequently reduced.

Alternative processes suppress the formation of bubbles by means of pulses or alternate currents/voltages. For example, Selvaganapathy et al.[11] describes the electro-kinetic pumping of species in aqueous-based solutions. He used an alternate sequence of positive and negative rectangular current pulses with the same charge but different height and time. There is a net displacement with time although the species move in an oscillating mode. Besra et al.[12] was able to obtain dense bubble-free deposits with EPD from an aqueous suspension. He used positive voltage pulses with the same on–off time. One year later, Neirinck et al.[13] proposed a process similar to that of Selvaganapathy et al.[11] He used, however, triangular voltage pulses. Dukhin and Dukhin[14] explained the reason for the suppression of bubbles with alternate currents combined with a net displacement of suspended particles. He described it as a non-linear dependence of the electrophoretic velocity of the particles when high electric fields are applied. Stotz[15] had already measured this non-linear dependence of the particle velocity and related it to the deformation of the particles double layer during their displacement.

In the case of Besra et al.[12] there is a resulting electric field, which is responsible for the particles movement. During the pulse off-time the bubble-formation precursors move back into the bulk of the electrolyte and their concentration is thus kept under the critical value. But only low deposition rates were attained in the pioneering works of Neirinck et al.[13] and Besra et al.[12] Furthermore, the Neirinck method requires high voltages to achieve a non-linear effect. But for suspensions with high electrical conductivity the high, dissipated power leads to an overheating of the suspension. Due to the high current density at point electrodes and, consequently, a high concentration of ions at the surface of the electrode, the Besra method can also not be applied.

In this work, a combination of both Besra and Neirinck methods was used. Thus it was possible to place the electrodes closer to each other and a better focusing of the electric field was achieved. Consequently, deposits with increased spatial resolution were obtained. To optimize the electrodes setup, model calculations of the local electric field distribution were performed.

2. Experimental setup

2.1. Simulation of electric fields

To achieve a small local deposit it is necessary to get a narrow electric field distribution. For that simulations (Comsol Multiphysics 3.5) of the electric field for different electrode setups were performed. Fig. 2 shows the plate and point electrodes setup (point electrode Ø = 500 μm, conductivity of both electrodes = 6×10^{17} S/m). In all cases, insulating boundaries were considered. A porous membrane (height 6 mm and 90 μm thick) was positioned in front of the plate electrode. The suspension is able to penetrate the pores. For simulation purposes, this changes the effective value of the membrane conductivity. An average (2.5×10^{-3} S/m) between the dry membrane conductivity (~0) and the suspension conductivity (5×10^{-3} S/m) was assumed. The distance d between the membrane and the point electrode was also varied.

2.2. Electrophoretic shaping process

The experimental setup with a plate and a point electrode (Ø = 500 μm) is shown in Fig. 3. A stainless steel plate electrode and a point electrode (90% Pt, 10% Rh) were used. The point electrode was covered with an electrically insulating coating, only the face section was not coated. As it was impossible to deposit directly on the stainless steel plate electrode, a porous membrane (Nadir, Carl Roth GmbH, Karlsruhe, Germany) or a graphite foil (Carbofles 98, 0.38 mm thick, Carbon Industrie-Produkte GmbH, Germany) were set in front of the plate electrode.

For the shaping process, a suspension consisting of 200 ml deionised water (σ = 0.9 μS/cm) and 40 g Al_2O_3-powder (SM8, Baikalox, d_{50} = 300 nm, BET = 10 m^2/g) was prepared. The conductivity and pH were adjusted adding 0.1 g of HNO_3 (6.5% diluted). The powder was dispersed in three steps: first, by means of a mini dissolver (Dispermat N1-SIP, VMA-GETZMANN

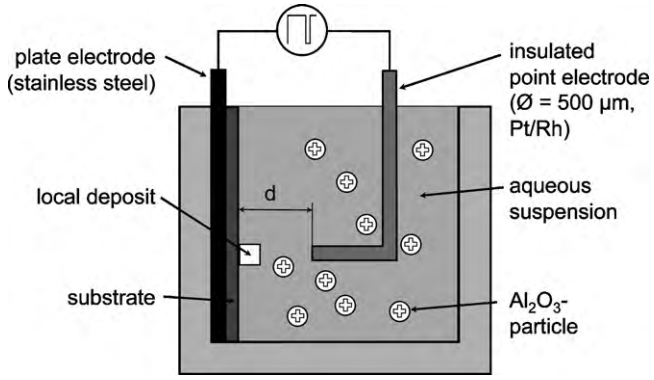

Fig. 3. Experimental setup with plate and point electrode for local deposition from Al_2O_3-suspension.

GmbH, Germany, disc diameter 32 mm) for 5 min at 30% of max. power, then with an ultrasonic dissolver (Sonifier W-450 D, G. HEINEMANN, Germany) for 15 min (pulse configuration: $t_{on} = 0.5$ s, $t_{off} = 0.5$ s, pulse amplitude = 20%) and, finally, again with the mini dissolver for 3 min at 30% of max. power. The dispersed suspension had a solid content of 16.6 wt.%, a pH of 5.8 and conductivity of 36 µS/cm. The suspended Al_2O_3-particles have a positive surface charge and therefore move towards the negative electrode.

The voltage pulses were programmed with an arbitrary waveform generator (33210A, Agilent Technologies). This generator allows for free programmable pulses with frequencies up to 10 MHz. An AC-amplifier (PAS 1000, Spitzenberger & Spies GmbH, Viechtach, Germany) was coupled to the generator. The amplifier maximum adjustable voltage is $\pm 382\ V_{DC}$, with a rise time >52 V/µs. The amplifier operates in DC and in AC mode up to a frequency of 5 kHz.

The applied voltage and resulting current were acquired with a DAQ Card (NI-6009 USB, National Instruments) and a LabView program. For long time observations, a sample rate of 2.25 kHz and a total of 135,000 samples (60 s) were used. When a higher resolution was required, a sample rate of 15 kHz and a total of 150,000 samples were recorded (10 s).

3. Results and discussion

3.1. Simulation of electric fields

The vertical dashed line in Fig. 2 marks the location lying 90 µm in front of the point electrode, along which the distribution of the electric-field-vector x-component for three different setups is plotted in Fig. 4. Here the dotted line corresponds to a plate and point electrode setup with a separation distance $d = 100$ µm between the membrane and the point electrode. This configuration presents the highest electric field peak favoring the best deposition rate.

The dashed line corresponds to a two point-electrodes configuration (both with diameter of 500 µm). A membrane of 90 µm thickness, onto which the powder was deposited, was placed between the point electrodes (this case is not shown in Fig. 2). Each electrode was positioned 100 µm away from the membrane. This setup has a lower electric field peak, but narrower distribution (better focusing) away from the point-electrode symmetry axis.

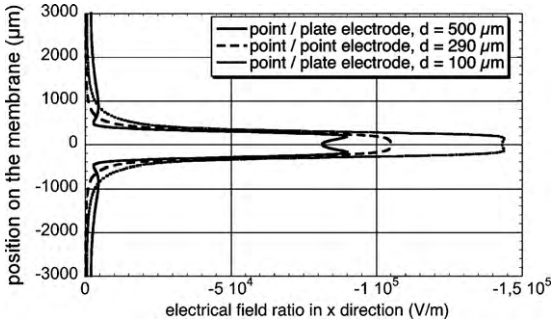

Fig. 4. Simulation results for three different electrode setups.

For manufacturing multilayer deposits, it is necessary to increase the distance between the electrodes. This scenario is shown with the continuous line (both plate and point electrodes are 500 µm away from each other) in Fig. 4. The electric field distribution has smaller peak value but, on the other hand, is narrower. Hence, it should allow the manufacturing of multilayer micro deposits.

3.2. Electrophoretic shaping process

The applied voltage pulse-shape is shown in Fig. 5. The areas under the positive and negative pulses are different. The ratio between V_2 and V_1 is 9 and t_1/t_2 is 4. As the negative pulse area A_2 is 2.5 times bigger than A_1, the particles move effectively towards the plate electrode instead of only oscillating about their rest positions. Due to the alternating voltage, the polarity of the electrodes is continuously varied and the concentration of reacting ions at the electrode surface is kept under the critical value needed for bubbles formation. Fig. 1 (Dinckelacker[10]) shows the dependence of the bubbles-formation time with the applied current density. Accordingly, to avoid generation of bubbles in our experimental setup, an increase in current density must be matched to an increase in applied pulse frequency.

In our case three different deposition times were applied: 7, 4 and 1 min, respectively. The employed frequencies were 150, 300 and 450 Hz. The distance d was 700, 400 and 200 µm and

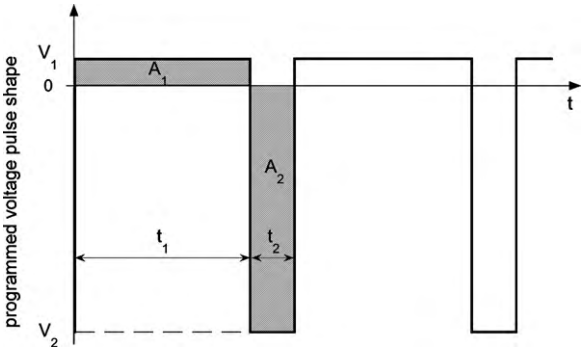

Fig. 5. Applied voltage signal in order to suppress bubbles formation, $V_2/V_1 = 9$, $t_1/t_2 = 4$, $A_2/A_1 = 2.5$.

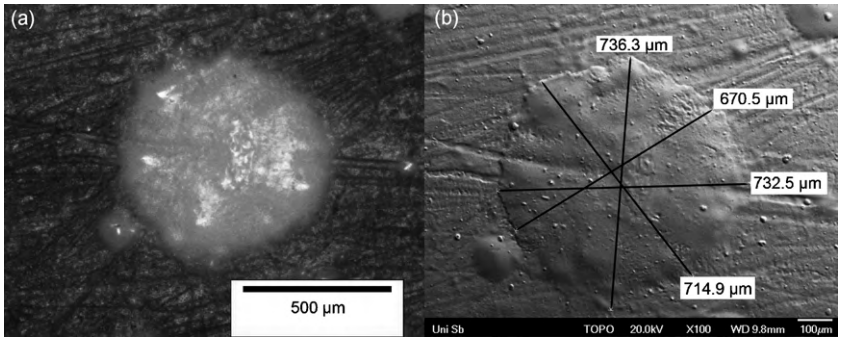

Fig. 6. Local deposit on a graphite foil, $t = 1$ min, $f = 450$ Hz, $V_1 = 1.929$ V, $V_2 = -17.361$ V, $d = 200$ µm: (a) microscope photo in wet condition, (b) SEM topographic picture after drying and sputtering with gold.

the voltages were $V_1 = 7.68$, 3.858 and 1.929 V and $V_2 = -69.12$, -34.722 and -17.361 V, respectively. The smallest bubble-free deposit obtained on a graphite foil ($t = 1$ min, $V_1 = 1.929$ V, $V_2 = -17.361$ V, $d = 200$ µm and $f = 450$ Hz) is shown in Fig. 6. Fig. 6(a) presents the wet deposit directly after the deposition. The deposit was dried in air, sputtered with gold and was observed in a SEM. The SEM micrograph in Fig. 6(b) shows several agglomerates on the deposit surface but no bubble channels can be seen. The diameter of the dried deposit varies from 670 to 736 µm, that is, only about 1.5 times bigger than the point electrode diameter.

In comparison to Fig. 6, where the deposit was obtained through application of a pulsed voltage, Fig. 7 presents the deposit obtained by applying a direct voltage. The same experimental parameters were used as for the deposit shown in Fig. 6, except for the application of a direct voltage of -17.3 V for 12 s. This time is the exact sum of the negative-peaks time within 1 min of the pulsed voltage experiment. The diameter of the obtained deposit (larger than 3 mm, see Fig. 7(a)) is clearly larger than the 736 µm obtained with the pulsed experiment. In an area from the middle of the deposit to the top of it, no deposition took place due to bubbles formation and their rising to the surface of the suspension. The zoom-in in Fig. 7(b) shows clearly the pore-channels formed by the bubbles generation. In comparison to the direct voltage deposition, the use of voltage pulses suppresses the formation of bubbles and reduces the deposit diameter.

The deposit pictured in Fig. 6 confirms the narrow distribution of the electric field as calculated in Fig. 4. The shape of the measured voltage pulses (Fig. 8(a)) differs slightly from the programmed one (Fig. 5) which means, that every third peak on the positive and negative pulse, there can be seen a supplementary peak that was not in the programmed voltage function. This is caused by the particles' inertia. During the fast voltage switch from negative to positive or vice versa the particles are accelerated very strongly so that as a consequence they are not able to slow down immediately during the constant voltage stage. This particles inertia leads to the current peaks observed in Fig. 8(b). Such peaks, according to the Ohm's law, must be followed by corresponding voltage peaks (Fig. 8(a)). This peaks should be seen on each pulse but appear only every third pulse due to the low sampling rate, which was limited by the DAQ Card. The current-to-voltage ratio is not linear. The voltage presents a constant value at the pulse plateau but the current decays slowly and does not show a pulse plateau.

The reason why deposition may be effected on a porous substrate (in this case membrane) and not on the non-porous steel electrode is still not clear in the EPD field. Our hypothesis is that during the deposition peak "A_2" the powder is still not strongly adsorbed to the non-porous substrate surface and then, during the peak "A_1" is desorbed again. In the case of the porous membrane, the powder particles may find suitable sites in the pores to anchor themselves strongly so that during the peak "A_1" will not be directed again into the suspension. After the first layer is successfully built, adsorption of a second layer is promoted due to the adsorption surface having now the same nature as the powder.

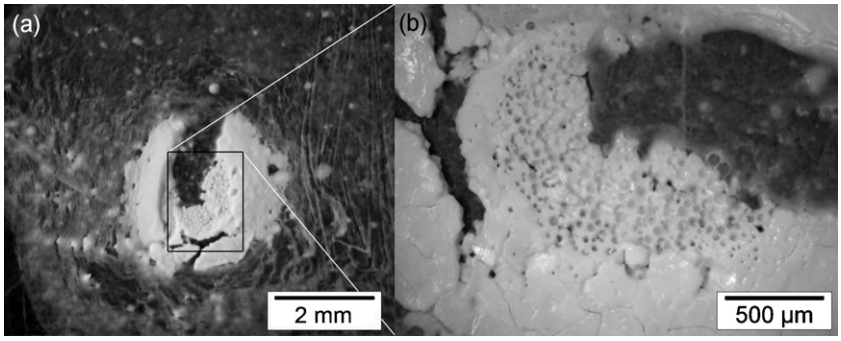

Fig. 7. Local deposit on a graphite foil, $t = 12$ s, constant voltage -17.361 V, $d = 200$ µm: (a) macro-photography of total deposit, (b) detailed cut-out with bubble pores.

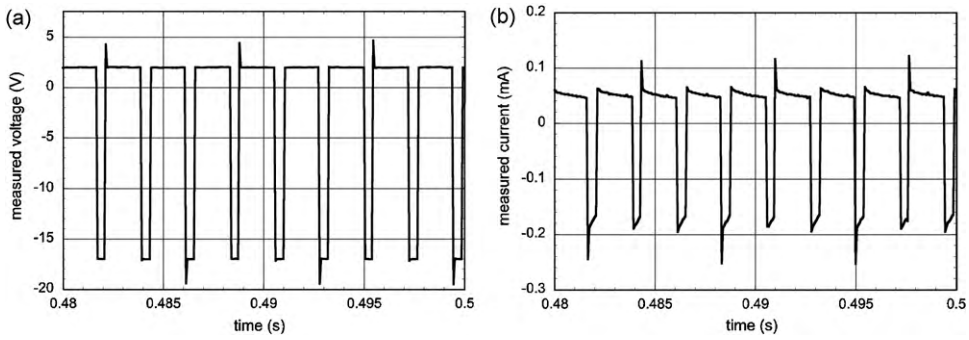

Fig. 8. Measured voltage (a) and current (b) during the deposition shown in Fig. 6, sample rate = 15 kHz.

4. Conclusions

In this work a new method to perform bubble-free local deposition from aqueous suspensions was demonstrated. To select the most suitable electrodes configuration, the electrical field distribution was simulated. An experimental setup was then arranged. The application of voltage pulses during deposition allowed to control the concentration of gas-producing ions at the electrode surface and thus to prevent the formation of bubbles. The different total area under the pulses caused the directional particle movement. The smallest bubble-free deposit was obtained on a graphite foil. Its diameter is only about 1.5 times bigger than the point electrode diameter. It is expected that deposits with even smaller dimensions should be obtained if smaller point electrodes and a closer configuration is used.

Acknowledgements

The authors would like to thank the German Research Foundation (DFG) for supporting this work under grant number CL 102/29-1. We would also like to thank Dr. R. Mayen-Mondragon for his support with the data acquisition issues.

References

1. Zeiner J, Nold A, Clasen R. Electrophoretic deposition as shaping technique – a CAM approach. *Adv Sci Technol* 2006;**45**:714–9.
2. Nold A. *Herstellung punkt- und linienförmiger Strukturen mittels EPD*. Saarbrücken: Studienarbeit, Universität des Saarlandes; 2006.
3. Assion T. *Untersuchungen zur EPD als Rapid Prototyping Verfahren*. Saarbrücken: Diplomarbeit, Universität des Saarlandes; 2006.
4. Zeiner J., *Untersuchungen zur Herstellung von Mikrostrukturen aus nanoskaligen Pulvern mittels elektrophoretischer Abscheidung*. Dissertation. Saarbrücken: Universität des Saarlandes; 2007.
5. Clasen R. Forming of compacts of submicron silica particles by electrophoretic deposition. In: Hausner H, Messing GL, Hirano S, editors. *2nd international conference on powder processing science*. Deutsche Keramische Gesellschaft: Köln. Berchtesgaden; 1988. p. 633–40.
6. Nold A, Zeiner J, Clasen R. Fast deposition of surface structures by two-step EPD. *Key Eng Mater* 2009;**412**:3–8.
7. Nold A, Zeiner J, Clasen R. Local electrophoretic deposition with coaxial electrodes. *Key Eng Mater* 2009;**412**:307–12.
8. Sakurada O, Suzuki K, Miura T, Hashiba M. Bubble-free electrophoretic deposition of aqueous zirconia suspensions with hydroquinone. *J Mater Sci* 2004;**39**:1845–7.
9. Lebrette S, Pagnoux C, Abélard P. Fabrication of titania dense layers by electrophoretic deposition in aqueous media. *J Eur Ceram Soc* 2006;**26**:2727–34.
10. Dinkelacker M., *Zur Gasentwicklung und Blasenbildung an Elektroden*. Dissertation. Stuttgart: Universität Stuttgart; 1989.
11. Selvaganapathy P, Ki YL, Renaud P, Mastrangelo CH. Bubble-free electrokinetic pumping. *J Microelectromech Syst* 2002;**11**:448–53.
12. Besra L, Uchikoshi T, Suzuki TS, Sakka Y. Bubble-free aqueous electrophoretic deposition (EPD) by pulse-potential application. *J Am Ceram Soc* 2008;**91**:3154–9.
13. Neirinck B, Fransaer J, Biest OVd, Vleugels J. Aqueous electrophoretic deposition in asymmetric AC electric fields (AC-EPD). *Electrochem Commun* 2009;**11**:57–60.
14. Dukhin AS, Dukhin DS. Aperiodic capillary electrophoresis method using an alternating current electric field for separation of macromolecules. *Electrophoresis* 2005;**26**:2149–53.
15. Stotz S. Field dependence of the electrophoretic mobility of particles suspended in low-conductivity liquids. *J Colloid Interface Sci* 1978;**65**:118–31.